

Liquids more stable than crystals

Frank Smallenburg and Francesco Sciortino

Department of Physics, Sapienza, Università di Roma, Piazzale Aldo Moro 2, I-00185, Roma, Italy

All liquids (except helium due to quantum effects) crystallize at low temperatures, forming ordered structures. The competition between disorder, which stabilizes the liquid phase, and energy, which favors the ordered crystalline structure, inevitably turns in favor of the latter when temperature is lowered and the entropic contribution to the free energy becomes progressively less and less relevant. The “liquid” state survives at low temperatures only as a glass, an out-of-equilibrium arrested state of matter. This textbook description holds inevitably for atomic and molecular systems, where the interaction between particles is set by quantum mechanical laws. The question remains whether the same physics hold for colloidal particles, where inter-particle interactions are usually short-ranged and tunable. Here we show that for patchy colloids with limited valence, conditions can be found for which the disordered liquid phase is stable all the way down to the zero-temperature limit. Our results offer interesting cues for understanding the stability of gels and the glass forming ability of atomic and molecular network glasses.

The ability to control — via chemical[1–3] or physical[4] patterning — the selectivity and angular flexibility of the inter-particle interaction[5] makes it possible to provide valence to colloids. Exploiting valence offers enormous possibilities, some of which have been addressed in recent years, theoretically [6] numerically[7–9] and experimentally[2, 10, 11]. Since colloidal interactions are typically short-ranged and thus limited to nearest neighbors, valence provides an implicit quantization of the particle energy, which becomes essentially proportional to the (limited) number of formed bonds. In an optimal arrangement, all particles bind with f neighbors and the system is in its lowest possible (ground) energy state. Typically, such an optimal arrangement is spatially ordered, defining the most stable crystal phase(s).

In principle, when density is not too high, it is possible to envision disordered optimal arrangements, in which all particles form exactly f bonds, giving rise to a disordered fully bonded structure which has exactly the same energy as the crystal. Under this unconventional condition, the stability of the system becomes controlled by its entropy, a case reminiscent of hard-sphere (HS) colloids, where crystal formation is observed despite the absence of any cohesive energy. In this study we demonstrate that the flexibility of the bond (encoded in the angular patch width) — a tunable quantity in the design of

patchy colloidal particles — is the key element in controlling the entropy of the liquid as compared to the one of the crystal. Large binding angles combined with limited valence give rise to thermodynamically stable, fully bonded liquids.

The model we consider is an extension of the widely used Kern-Frenkel model[12] for patchy particles, where we explicitly enforce a single-bond-per-patch condition. Each spherical particle of diameter σ has f circular attractive patches on its surface, characterized by an opening angle θ_m . Two particles are bonded with a fixed bonding energy ϵ when their center-to-center distance is smaller than the interaction range $\sigma + \delta$, and the vector connecting the particles passes through a patch on both particles (see Supplementary Information (SI)). We examine a mono-disperse systems of particles with $f = 4$ attractive patches, arranged in a tetrahedral configuration, mimicking recently synthesized colloids[2]. The values of δ and θ_m fix the volume available for bonding V_b .

The phase diagrams, evaluated using free-energy calculations, for different θ_m are shown in Fig. 1 as a function of density ρ and T . The phases appearing in Fig. 1 include, besides the disordered gas and liquid phases, a diamond cubic crystal phase, a body-centered cubic (BCC) crystal phase, consisting of two interlocking diamond lattices, and a face-centered cubic (FCC) crystal phase, where, for sufficiently narrow patches, the bonds are periodically ordered at low T and disordered at high T . All these crystals are fully bonded at low T .

For narrow patch width, the phase diagram closely resembles the standard phase diagrams with a triple point below which the liquid state ceases to exist. Unexpectedly, for wider patches the open diamond crystal phase disappears from the phase diagram and a region in which the liquid is stable down to vanishing T opens up at intermediate ρ , in agreement with a numerical study of DNA-coated colloids[9, 14]. In this range of densities, the liquid is the phase with the lowest free energy, despite its intrinsic long range disorder. Increasing the patch width even further reduces the region of stability for the BCC and the disordered FCC crystals. For very wide patches, the phase diagram simply consists of gas, liquid, and FCC crystal phases, with a large stable liquid region even in the zero-temperature limit.

Why is the liquid more stable than the crystal? Figure 2 shows the T dependence of the number of bonds per particle n_b for different θ_m . Upon cooling, n_b increases continuously to four, while the system progressively approaches the fully bonded random tetrahedral network state, the ground state of the system. Configurations

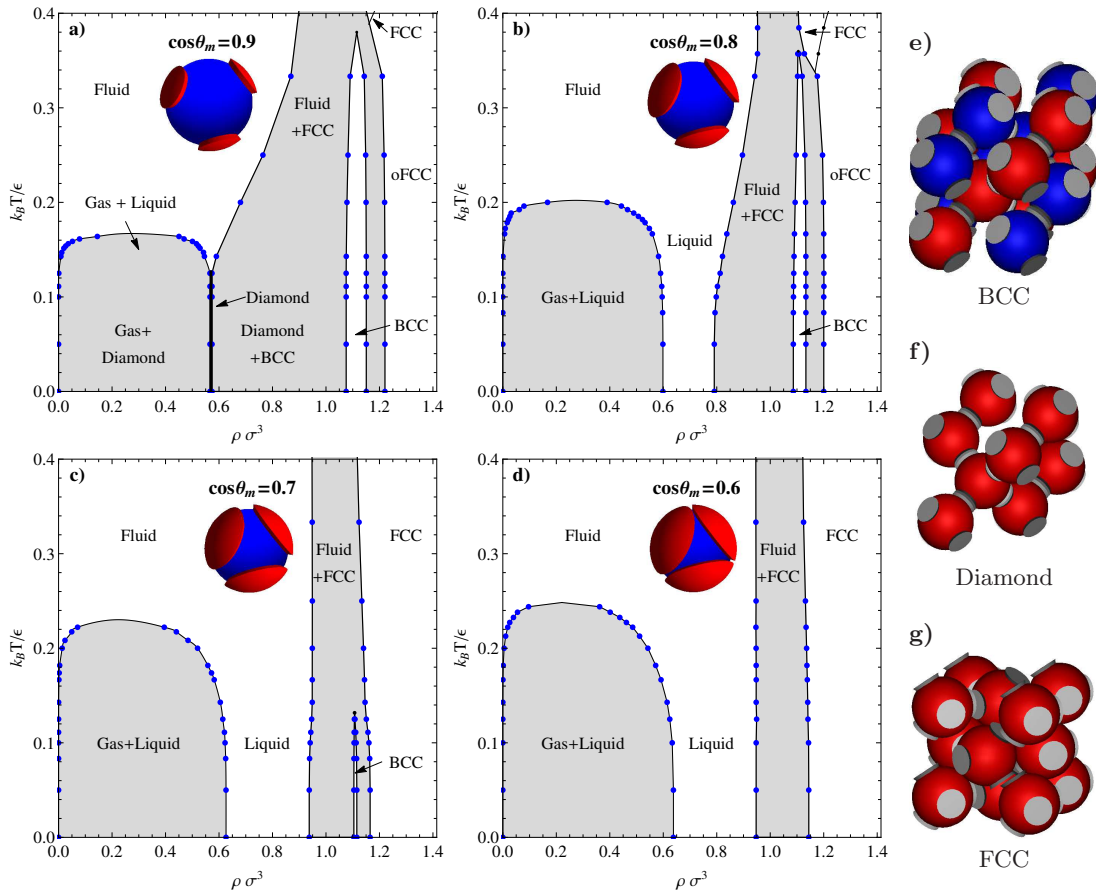


FIG. 1: **Phase diagram of tetrahedral coordinated patchy colloids for different patch widths.** (a) $\cos\theta_m = 0.9$, (b) $\cos\theta_m = 0.8$, (c) $\cos\theta_m = 0.7$, and (d) $\cos\theta_m = 0.6$. Data are reported in dimensionless density ($\rho\sigma^3$) and temperature $k_B T/\epsilon$, where k_B is the Boltzmann constant. The interaction range in all cases is fixed at $\delta = 0.12\sigma$, a value typical of colloidal interactions. Narrower patches ($\cos\theta_m > 0.9$) behave as the $\cos\theta_m = 0.9$ case[13] and are not shown here. The gray areas denote coexistence regions and the points denote calculated coexisting states (tie lines are horizontal). The points below $k_B T/\epsilon = 0.1$ are based on extrapolation of the potential energy. The label oFCC denotes the orientationally ordered face-centered cubic phase, while the disordered FCC phase is simply denoted as FCC. The pictures on the right show the unit cell of BCC (e), with the two interspersed diamond lattices indicated in different colors, diamond (f) and orientationally ordered FCC (g).

with $n_b = 4$ are indeed sampled during the numerical runs. At low T , the potential energy of the liquid is thus equal to that of the crystals. Hence, the stability of the liquid, as in the HS case, results from a subtle competition between vibrational S_{vib} and configurational S_{conf} components of the total entropy $S_{\text{tot}} = S_{\text{vib}} + S_{\text{conf}}$ [15, 16]. S_{vib} measures the (phase-space) volume explored by each particle in a fixed bonding topology, and is larger in the ordered structure than in the fluid. S_{conf} measures the number of distinct configurations resulting in a fully bonded macroscopic state. It vanishes in the crystals and is positive in the fluid phase. Both quantities can be calculated as discussed in the methods section.

Figure 3a shows how the patch width affects the entropy. Similar to dense HS, S_{vib} in the diamond structure ($S_{\text{vib}}^{\text{DC}}$) is always larger than in the liquid ($S_{\text{vib}}^{\text{liq}}$).

Hence in the disordered phase each particle is more constrained than in the ordered one. If S_{vib} would be the only source of entropy, the diamond would be the stable phase at all θ_m . However, the entropy of the liquid is enhanced by S_{conf} , causing for wide angles the unconventional stability of the liquid phase even when $T \rightarrow 0$. In this large θ_m region, the model provides a neat example of a system for which the Kauzmann temperature (T_K)[16] does not exist. Indeed, S_{conf} (Fig. 3b) does not vanish when $T \rightarrow 0$. For small θ_m , extrapolations suggest that a finite T_K could exist, but its detection is preempted by dynamic arrest and/or crystallization (as commonly found in atomic or molecular systems). Thus, for wide patches, a previously unexplored thermodynamically stable state of matter arises: the disordered fully bonded network. We note that while our results are for

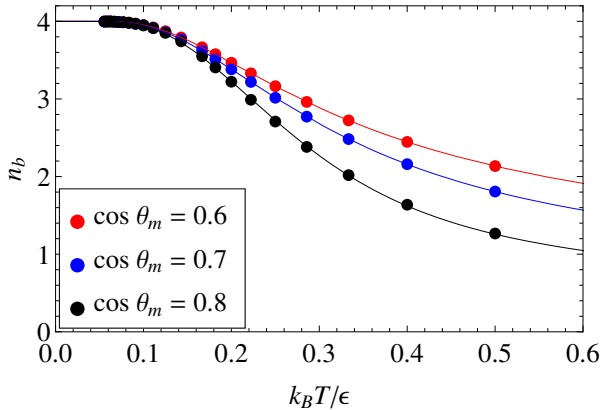


FIG. 2: **Number of bonds per particle in the liquid phase.** Here $\rho\sigma^3 = 0.57$, the same density of the diamond crystal phase. In the zero-temperature limit, the number of bonds per particle n_b reaches the maximum of 4. Points denote measurements in NVT simulations, and lines are fits to guide the eye. Note that the approach to the ground state ($n_b = 4$) takes place at higher T for large θ_m values, a result induced by the larger bonding volume.

$f = 4$, it is reasonable to expect that zero-temperature liquids will also occur in systems with a different (but small) f , assuming a large patch angle. Our results provide a clear framework for understanding the microscopic origins of the observed difficulties of crystallizing DNA-coated colloids when valence is small[9, 14]. We also stress the relevance of our predictions for the colloidal realm [1, 2, 9, 14] where bonding rigidity is largely dominated by entropic effects and bonds do not become less flexible upon decreasing T . This fact is crucial in maintaining a finite S_{conf} in the low- T limit and explains why the fully bonded network state does not occur in atomic or molecular systems, where θ_m decreases on cooling.

To provide further evidence that sampling of the fully bonded state is not pre-empted by dynamic arrest and to characterize the low T dynamics we investigate the microscopic mechanism associated with the evolution of the network. We start by focusing on the defects of the fully bonded network (broken bonds), which act as elementary diffusing units. At any T close to zero the number of broken bonds per particle (α_{bb}) depends on T as $\exp(-\epsilon/2k_B T)$, as demonstrated in the SI. Fig. 4a shows that α_{bb} indeed satisfies the exponential T dependence for all θ_m . We observe two different mechanisms for restructuring the network at low T : bond-breaking and bond-switching, depending on θ_m . For small θ_m the single-bond-per-patch condition is automatically implemented by geometric constraints[6] and hence bonds must first break and then reform with new (or identical) partners. For large θ_m the bonding volumes of different neighbors can overlap and the switching of bonds with no energetic penalty allows the system to relax stresses

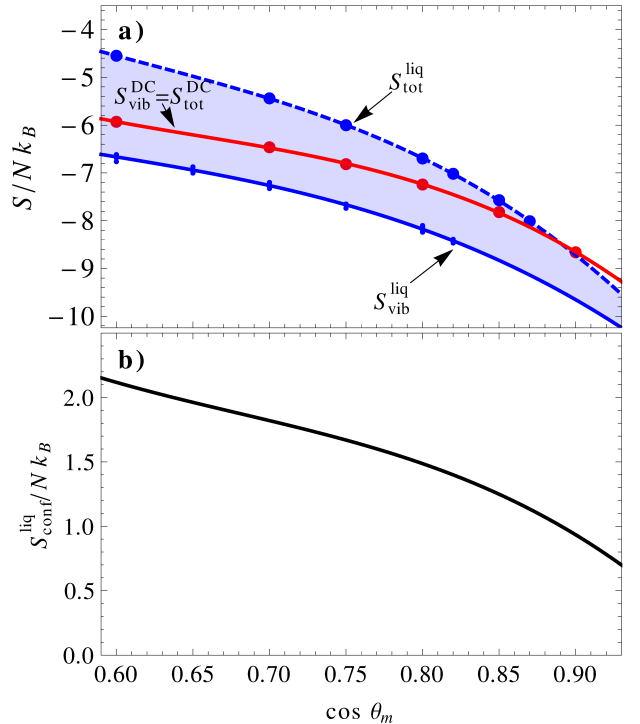


FIG. 3: **Total, vibrational, and configurational entropy for the zero-temperature phases.** Here $\rho\sigma^3 = 0.57$. **a)** The vibrational and total entropy for the diamond crystal (DC) and liquid (liq) phases. For the diamond crystal, the total entropy $S_{\text{tot}}^{\text{DC}}$ coincides with the vibrational entropy $S_{\text{vib}}^{\text{DC}}$. Below $\cos\theta_m \approx 0.89$, the fully bonded liquid becomes more stable than the crystal. For each angular patch width θ_m , five independent $S_{\text{vib}}^{\text{liq}}$ calculations are shown. Lines are polynomial fits to the points. With extremely lengthy simulations fully bonded configurations can be sampled up to $\cos\theta_m = 0.92$. Note that the entropies are negative since we are investigating a classical system and the (constant) kinetic contribution is not included. **b)** Configurational entropy $S_{\text{liq}}^{\text{conf}}$ of the liquid at $T \rightarrow 0$, calculated as the difference between the fits for $S_{\text{tot}}^{\text{liq}}$ and $S_{\text{vib}}^{\text{liq}}$.

relatively quickly. The bond-switching mechanism mimics the microscopic dynamics of vitrimers[17], a recently invented malleable network plastic where a catalyst enables the switching (transesterification) of bonds between nearby polymers.

To quantify the low T dynamics we perform event driven molecular dynamics (EDMD) simulations and examine the diffusion coefficient D at low T . Results are reported in Fig. 4b. For wide patches, D follows an Arrhenius law, with an activation energy of $\epsilon/2$, the same as α_{bb} . D is thus proportional to the number of broken bonds, demonstrating that switching between broken and formed bonds is the key element in the microscopic dynamics. For patch widths such that bond switching is not a viable mechanism ($\cos\theta_m \geq 0.89$), D still follows an Arrhenius law, but with an activation energy of 2ϵ , i.e.

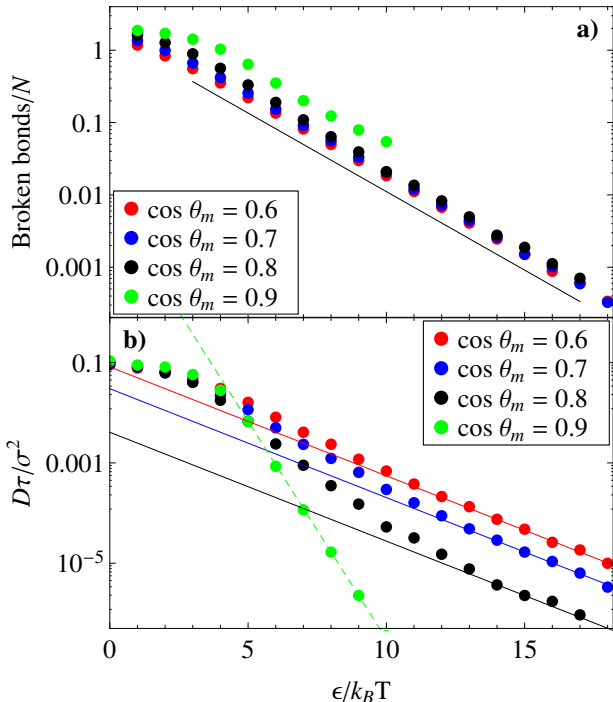


FIG. 4: **Defects of the fully bonded network and their dynamic role.** **a)** The number of broken bonds per particle α_{bb} as a function of the inverse temperature $\epsilon/k_B T$, for different patch widths, at constant density $\rho\sigma^3 = 0.65$. The line has slope $-1/2$. **b)** The (a -dimensional) diffusion coefficient D as a function of the inverse temperature $\epsilon/k_B T$. In the EDMD, an attempt to break, form or switch bond is performed with a rate γ . Data here refer to a constant bond switching rate $\gamma\tau = 100$, a value for which the dynamics is not affected by the specific value of γ (see SI). The lines have slopes $-1/2$ (for $\cos\theta_m = 0.6, 0.7, 0.8$) and slope -2 (for $\cos\theta_m = 0.9$).

four times the corresponding value for α_{bb} . This functional dependence is the same as the one that quantifies the number of particles with four broken bonds, i.e. particles completely detached from the network. This suggests that — consistent with previous results of the slow dynamics of models of water[18] and other tetrahedral networks[19, 20] — the diffusion of these rare particles dominates the microscopic dynamics.

Independently from the microscopic dynamics, D always vanishes following the Arrhenius behavior characteristic of strong atomic and molecular network forming liquids. The activation energy value (which can vary up to a factor of four) encodes information about the dominant microscopic mechanism.

In summary, our calculations clearly show that patchy colloids with a limited number of flexible bonds smoothly transform from a liquid to a fully bonded network, via the progressive reduction of the number of network defects, without the intervention of a more stable crystal phase or phase separation. Counterintuitively, the low

T phase behavior is governed by entropy, rather than energy, as all competing phases reach the ground state. The main requirements for the existence of a stable liquid at low T are thus a large flexibility of the interparticle bonds and a low valence. The large patch width ensures that a wide variety of network realizations can be formed. This configurational entropy is instrumental in stabilizing the liquid phase with respect to the crystal. The low valence ensures that the density of the liquid coexisting with the gas is small[6], leaving a large density region where the network can form. Both are key ingredients for the formation of what can be considered a previously unexplored state of matter: the thermodynamically stable fully bonded network state.

METHODS SUMMARY

Model

We consider an extension of the Kern-Frenkel model[12], where each patch can form at most one bond (see Fig. 5). In the normal Kern-Frenkel model, two patchy particles i and j , located at \mathbf{r}_i and \mathbf{r}_j respectively, feel an attraction given by

$$u_{\text{patch}}(i, j) = u_{\text{sw}}(r_{ij})\Phi(\mathbf{r}_{ij}, \{\mathbf{p}_i\})\Phi(\mathbf{r}_{ji}, \{\mathbf{p}_j\}) \quad (1)$$

where $\mathbf{r}_{ij} = \mathbf{r}_j - \mathbf{r}_i$, $\{\mathbf{p}_i\}$ is set of normalized vectors pointing from the center of particle i towards each of its patches, and u_{sw} is a square-well potential of hard diameter σ , range δ and depth ϵ .

$$\beta u_{\text{sw}}(r) = \begin{cases} \infty & \text{if } r < \sigma \\ -\beta\epsilon & \text{if } \sigma \leq r < \sigma + \delta \\ 0 & \text{otherwise} \end{cases} \quad (2)$$

Here, $\beta = 1/k_B T$, with k_B Boltzmann's constant.

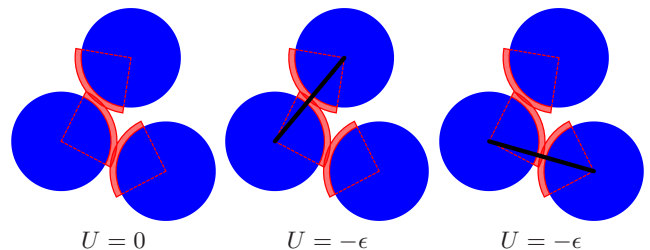


FIG. 5: **Cartoon of the interaction between patchy particles.** In the configuration on the left, three particles are close enough together to bond, but unbonded (potential energy $U = 0$). In the next two configurations, the two different bonding possibilities between the particles are shown, both with potential energy $U = -\epsilon$. In this case, at most one bond can be formed.

The function $\Phi(\mathbf{r}_{kl}, \{\mathbf{p}_k\})$ is defined as

$$\Phi(\mathbf{r}, \{\mathbf{p}\}) = \begin{cases} 1 & \text{if } \hat{\mathbf{r}} \cdot \hat{\mathbf{p}} > \cos(\theta_m) \text{ for any } \mathbf{p} \text{ in } \{\mathbf{p}\} \\ 0 & \text{otherwise} \end{cases} \quad (3)$$

In short, two particles bond if the vector connecting the centers of the particles passes through an attractive patch on each of the surfaces of each particle. Hence, as long as the patches on the same particle do not overlap, the Kern-Frenkel model only allows for a single bond between two particles. However, a single patch can make a bond with multiple different nearby particles if the patch width is larger (for our δ) than 0.895.

Here, we propose and implement (see SI) a modification to the Kern-Frenkel model that allows only one bond per patch for all θ_m values. In this modification, the overlap of the bonding volumes is not a sufficient criterium for defining the presence of a bond.

Methods

To calculate the free energy of the various phases as a function of the density, we use thermodynamic integration over the equation of state[21], as measured using Event-driven Molecular Dynamics (EDMD) simulations. For the gas, the reference state is an ideal gas. For the liquid, and fluids above the critical point, the hard-sphere fluid is used as a reference state, integrating over the well depth ϵ at fixed density. Similarly, the hard-sphere crystal was used as a reference state for the disordered FCC crystal. We use the Frenkel-Ladd method to calculate free energies of the diamond, BCC, and ordered FCC crystal structures[22], using an additional aligning potential to fix the orientation of the particles[23]. Finally, we determine phase coexistence using a common-tangent construction, and use the resulting coexistence points to draw the phase diagram.

For the calculation of the total entropy S_{tot} at $T = 0$, we use thermodynamic integration over the temperature. As the potential energy of all phases decreases exponentially at low temperatures, extrapolation to zero temperature is straightforward, and integrating over the exponential decay allows us to directly calculate the entropy at $T = 0$. The common tangent constructions at zero temperature are shown in the SI.

To calculate the vibrational entropy S_{vib} in the liquid phase, we use the Frenkel-Ladd method on a fully bonded configuration taken from a simulation at low temperature. The network topology is kept fixed during the calculation. To reduce the maximum spring constant required in the integration, we first “optimize” the configuration in a separate MC simulation biased towards configurations where small displacements of particles do not cause overlaps or break bonds. See the SI for more information.

We use EDMD simulations for calculating the equations of state and potential energies required for thermodynamic integration, and to investigate the dynamics of the low-temperature liquid phase[? ?]. For a full description of the implementation of the Kern-Frenkel model in EDMD simulations, see the SI. For all EDMD simulations used here, the simulation box is chosen to be cubic or rectangular, with periodic boundary conditions. The simulations are performed at fixed number of particles N , volume V , and temperature T . The temperature is regulated by means of a thermostat: at regular intervals, a random particle is given a new velocity and angular velocity, drawn from a Maxwell-Boltzmann distribution. Time is measured in units of $\tau = \sqrt{\beta m \sigma^2}$, with m the mass of a particle. For the simulations in this study, we chose the moment of inertia $I = m \sigma^2$. Note that the choice of mass or moment of inertia has no effect on the equilibrium phase behavior. Bond switching moves in the EDMD simulation (see SI) are events that happen at a fixed rate γ for each patch in the system, such that per time unit τ each patch experiences $\gamma\tau$ attempts to form, switch, or break a bond. Diffusion coefficients were obtained from the slope of the mean squared displacement as a function of time. The system sizes (ranging from $N = 512$ to 64000) were chosen to ensure that the number of broken bonds in the system would be at least one on average, for the temperatures under consideration.

-
- [1] Chen, Q., Bae, S. C. & Granick, S. Directed self-assembly of a colloidal kagome lattice. *Nature* **469**, 381–384 (2011).
 - [2] Wang, Y. *et al.* Colloids with valence and specific directional bonding. *Nature* **491**, 51–55 (2012).
 - [3] Pawar, A. B. & Kretzschmar, I. Fabrication, assembly, and application of patchy particles. *Macromol. Rapid Comm.* **31**, 150–168 (2010).
 - [4] Kraft, D. J. *et al.* Surface roughness directed self-assembly of patchy particles into colloidal micelles. *Proc. Natl. Acad. Sci. U.S.A.* **109**, 10787–10792 (2012).
 - [5] Glotzer, S. C. & Solomon, M. J. Anisotropy of building blocks and their assembly into complex structures. *Nature Mater.* **6**, 557 (2007).
 - [6] Bianchi, E., Largo, J., Tartaglia, P., Zaccarelli, E. & Sciortino, F. Phase diagram of patchy colloids: Towards empty liquids. *Phys. Rev. Lett.* **97**, 168301 (2006).
 - [7] de las Heras, D., Tavares, J. M. & M. M. Telo da Gama. Bicontinuous and mixed gels in binary mixtures of patchy colloidal particles. *Soft Matter* **8**, 1785–1794 (2012).
 - [8] Sciortino, F. Gel-forming patchy colloids and network glass formers: thermodynamic and dynamic analogies. *Eur. Phys. J. B* **64**, 505–509 (2008).
 - [9] Martinez-Veracoechea, F. J., Mladek, B. M., Tkachenko, A. V. & Frenkel, D. Design rule for colloidal crystals of dna-functionalized particles. *Phys. Rev. Lett.* **107**, 079902 (2011).
 - [10] Ruzicka, B. *et al.* Observation of empty liquids and equi-

- librium gels in a colloidal clay. *Nature Mater.* **10**, 56–60 (2011).
- [11] Biffi, S. *et al.* Phase behaviour and critical activated dynamics of limited-valence dna nano-stars. *Submitted* (2013).
- [12] Kern, N. & Frenkel, D. Fluid–fluid coexistence in colloidal systems with short-ranged strongly directional attraction. *J. Chem. Phys.* **118**, 9882–9889 (2003).
- [13] Romano, F., Sanz, E. & Sciortino, F. Phase diagram of a tetrahedral patchy particle model for different interaction ranges. *J. Chem. Phys.* **132**, 184501 (2010).
- [14] Martinez-Veracoechea, F. J., Bozorgui, B. & Frenkel, D. Anomalous phase behavior of liquid-vapor phase transition in binary mixtures of dna-coated particles. *Soft Matter* **6**, 6136–6145 (2010).
- [15] Moreno, A. J. *et al.* Energy landscape of a simple model for strong liquids. *Phys. Rev. Lett.* **95**, 157802 (2005).
- [16] Debenedetti, P. G. & Stillinger, F. H. Supercooled liquids and the glass transition. *Nature* **410**, 259–267 (2001).
- [17] Montarnal, D., Capelot, M., Tournilhac, F. & Leibler, L. *Science* **334** (2011).
- [18] Poole, P. H., Becker, S. R., Sciortino, F. & Starr, F. W. Dynamical behavior near a liquid-liquid phase transition in simulations of supercooled water. *J. Phys. Chem. B* **115**, 14176–14183 (2011).
- [19] De Michele, C., Gabrielli, S., Tartaglia, P. & Sciortino, F. Dynamics in the presence of attractive patchy interactions. *J. Chem. Phys. B* **110**, 8064–8079 (2006). PMID: 16610908.
- [20] Largo, J., Starr, F. W. & Sciortino, F. Self-Assembling DNA Dendrimers A Numerical Study. *Langmuir* **23**, 5896–5905 (2007).
- [21] Frenkel, D. & Smit, B. *Understanding Molecular Simulations: From Algorithms to Applications* (Academic Press, San Diego, 2002).
- [22] Frenkel, D. & Ladd, A. J. C. New Monte Carlo method to compute the free energy of arbitrary solids. Application to the fcc and hcp phases of hard spheres. *J. Chem. Phys.* **81**, 3188–3193 (1984).
- [23] Noya, E. G., Vega, C., Doye, J. P. K. & Louis, A. A. Phase diagram of model anisotropic particles with octahedral symmetry. *J. Chem. Phys.* **127**, 054501 (2007).

ACKNOWLEDGEMENTS

We acknowledge support from ERC-226207-PATCHYCOLLOIDS. We thank F. Romano for useful discussions.